

Published in final edited form as:

Biochemistry. 2007 November 20; 46(46): 13415–13424. doi:10.1021/bi700774s.

## The kinetics of Ca<sup>2+</sup>-dependent switching in a calmodulin-IQ domain complex

DJ Black, J. Eva Selfridge, and Anthony Persechini<sup>‡</sup>

Division of Molecular Biology and Biochemistry, University of Missouri-Kansas City, Kansas City, Missouri 64110-2499

### Abstract

We have performed a kinetic analysis of Ca<sup>2+</sup>-dependent switching in the complex between calmodulin (CaM) and the IQ domain from neuromodulin, and have developed detailed kinetic models for this process. Our results indicate that the affinity of the C-ter Ca<sup>2+</sup>-binding sites in bound CaM is reduced due to a ~10-fold decrease in the Ca<sup>2+</sup> association rate, while the affinity of the N-ter Ca<sup>2+</sup>-binding sites is increased due to a ~3-fold decrease in the Ca<sup>2+</sup> dissociation rate. Although the Ca<sup>2+</sup>-free and Ca<sup>2+</sup>-saturated forms of the CaM-IQ domain complex have identical affinities, CaM dissociates ~100 times faster in the presence of Ca<sup>2+</sup>. Furthermore, under these conditions CaM can be transferred to the CaM-binding domain from CaM kinase II via a ternary complex. These properties are consistent with the hypothesis that CaM bound to neuromodulin comprises a localized store that can be efficiently delivered to neuronal proteins in its Ca<sup>2+</sup>-bound form in response to a Ca<sup>2+</sup> signal.

At some level, all physiological responses involve coordinated biochemical changes triggered by intracellular Ca<sup>2+</sup> signals. The Ca<sup>2+</sup>-binding protein calmodulin (CaM<sup>1</sup>), which engages in modulatory interactions with more than 100 known target proteins, is the primary mediator of Ca<sup>2+</sup>-dependent biochemical changes. Although many CaM targets, such as phosphodiesterase, myosin light chain kinase and the constitutive nitric oxide synthases do not interact significantly with the Ca<sup>2+</sup>-free protein (1–4), a large class bind Ca<sup>2+</sup>-free CaM at least as well as the Ca<sup>2+</sup>-bound forms of the protein. The majority of these, including neuromodulin, neurogranin, the unconventional myosins and some Ca<sup>2+</sup>, K<sup>+</sup> and Na<sup>+</sup> channels, interact with CaM via IQ domains, which have the consensus sequence: [I,L,V]QxxxR[G,x]xxx[R,K] (5–8). These regions bind apoCaM and/or Ca<sup>2+</sup>-bound CaM with dissociation constants ranging from subnanomolar to micromolar, depending upon their precise sequence and context (6). Complexes between CaM and IQ domains have been demonstrated to participate in a variety of regulatory processes, including positive and negative modulation of ion channels and unconventional myosin based motility (6). Some IQ domain proteins have been proposed to provide localized intracellular stores of CaM (9). The potential significance of such stores has

<sup>‡</sup>To whom all correspondence should be addressed: Division of Molecular Biology and Biochemistry, University of Missouri-Kansas City, 5007 Rockhill Road, Kansas City, MO 64110-2499, Tel 816-235-6076; Fax 816-235-5595; Email: Persechinia@umkc.edu.

<sup>†</sup>This work was supported by NIH Grant GM074887 to A.P.

#### <sup>1</sup>Abbreviations

CaM, calmodulin; BSCaMIQ, fluorescent biosensor containing a CaM-binding sequence based on the IQ domain in neuromodulin; ECFP, cyan emitting variant of green fluorescent protein, EYFP<sub>C</sub>, yellow emitting variant of green fluorescent protein; N<sub>x</sub>CCaM, mutant CaM with E31A and E67A substitutions; NC<sub>x</sub>CaM, mutant CaM with E104A and E140A substitutions; N-ter, the NH<sub>2</sub>-terminal end of a polypeptide; C-ter, the COOH-terminal end of a polypeptide; NC, Ca<sup>2+</sup>-free CaM; N<sub>2</sub>C, CaM with Ca<sup>2+</sup> bound to both N-ter EF hands; NC<sub>2</sub>, CaM with Ca<sup>2+</sup> bound to both C-ter EF hands; N<sub>2</sub>C<sub>2</sub>, CaM with Ca<sup>2+</sup> bound to all four EF hands; BAPTA, 1,2-bis(2-aminophenoxy)ethane-N,N,N',N'-tetraacetic acid; dibromo-BAPTA, 1,2-bis(2-amino-5,5'-dibromophenoxy)ethane-N,N,N',N'-tetraacetic acid; FRET, fluorescence resonance energy transfer; ckPEP, a synthetic peptide based on the CaM-binding domain in CaM-dependent protein kinase II; ngPEP, a synthetic peptide based on the CaM-binding domain in neurogranin.

been highlighted by recent investigations demonstrating that the intracellular CaM concentration can be limiting (10–12). Neuromodulin, a neuronal IQ domain protein found in axons and terminals, is perhaps the best studied example of such a protein (9). Neurogranin, a smaller protein with an essentially identical IQ domain, is thought to perform a similar function in dendritic spines (13,14).

The results presented in this paper indicate that the properties of the neuromodulin CaM-IQ domain complex promote dissociation of CaM in its Ca<sup>2+</sup>-bound form, and allow it to be transferred to target proteins via a ternary complex. These features are conducive to the efficient delivery of Ca<sup>2+</sup>-bound CaM to target proteins. Our results also demonstrate that the association rate constant for the C-ter EF pair of Ca<sup>2+</sup>-binding sites in CaM is reduced by a factor of ~10 in the IQ domain complex. This somewhat novel finding is consistent with the accompanying reduction in the affinity of the complex (15). The detailed kinetic models that we present for Ca<sup>2+</sup>-dependent switching in this complex may be applicable to CaM-IQ domain complexes in proteins where Ca<sup>2+</sup>-dependent switching appears to directly modulate function, such as ion channels and unconventional myosins (5–8).

## Materials and Methods

### Proteins

The composition, expression and purification of the fluorescent reporter, BSCaM<sub>IQ</sub>, have been described in detail elsewhere (15), as have the methods used to express and purify native and mutant CaMs (16,17). The two mutant CaMs used in these studies are N<sub>x</sub>CCaM, in which glutamic acid residues at positions 31 and 67 in the N-ter EF-hands have been replaced by alanines, and NC<sub>x</sub>CaM, in which the homologous glutamic acid residues at positions 104 and 140 have been replaced. As designated by the “x” subscript, these mutations eliminate Ca<sup>2+</sup> binding to the N-ter or C-ter EF hand pair. Two synthetic peptides were used in these studies. One, termed ckPEP, is based on the CaM-binding domain in CaM-dependent protein kinase II and has the sequence: MHRQETVDCLKKFNARRKLGAILTTMLA (Calbiochem, San Diego, CA). The other, termed ngPEP, is based on the IQ domain in neurogranin and has the sequence: AAKIQASFRGHMARKK (Promega, Madison, WI).

### Stopped-flow fluorescence measurements

All dynamic fluorescence measurements were performed using an SX18-MV Stopped-Flow Reaction Analyzer with a nominal ~1.4 ms dead time (Applied Photophysics, Leatherhead, UK). Excitation light from a 75 watt xenon arc lamp is supplied via a fiber optic-coupled monochromator (5 nm slit widths). Fluorescence emission is monitored using a high voltage PMT fitted with an appropriate absorbance filter. To monitor changes in FRET between ECFP and EYFP<sub>C</sub> in BSCaM<sub>IQ</sub>, ECFP fluorescence was excited at 430 nm and EYFP<sub>C</sub> emission was monitored using an LG535 long-pass absorbance filter (Corion, Franklin, MA). Ca<sup>2+</sup>-dependent changes in quin-2 fluorescence excited at 330 nm were monitored using an LG505 long pass emission filter. In experiments where quin-2 or CaM-binding peptides were used to trap Ca<sup>2+</sup> or CaM, a range of quin-2 or peptide concentrations were examined to ensure the absence of rebinding. All progress curves presented are the average of at least 6 individual determinations. Reactions were initiated by rapidly mixing equal volumes of reactant solutions to produce the stated final reactant concentrations. The base experimental buffer contained 25 mM Tris; pH 7.5, 0.1 M KCl and 100 µg/ml BSA, with other components as specified in the text or captions. Where indicated, proteins and buffers were decalcified by successive treatments with Chelex<sup>TM</sup> and a BAPTA-polystyrene column (Molecular Probes, Inc.). Contaminating amounts of Ca<sup>2+</sup> in decalcified protein solutions were 50 nM or less, based on the absence of any detectable effect on the A<sub>263</sub> of BAPTA. Stopped-flow experiments were performed at 22 °C.

## Analysis and modeling of kinetic data

Rate constants were derived from fits of individual fluorescence time courses to mono or double exponentials or from global fits of multiple time courses to explicit kinetic models performed using the Dynafit program (18). Standard errors given for the fitted parameters are the square roots of the diagonal elements in the variance-covariance matrices calculated for the non-linear least squares fits. In order to perform global fitting to explicit models it was necessary to assign relative molar fluorescence amplitudes to all kinetic species so as to account for their contributions to observed fluorescence. Values of 1.0 and 0.68 were assigned to free BSCaM<sub>IQ</sub> and the Ca<sup>2+</sup>-free CaM-BSCaM<sub>IQ</sub> complex, and values of 0.83 and 0.85 were assigned to the Ca<sup>2+</sup>-saturated complex and the intermediate complexes in which one CaM EF hand pair or the other is Ca<sup>2+</sup>-saturated. These values were previously determined under equilibrium conditions, and were validated in the stopped-flow fluorometer (15). Occupancy of an EF hand pair by only a single Ca<sup>2+</sup> ion was assumed to have no effect on fluorescence, because fluorescence changes observed under equilibrium conditions appear to require occupancy of both Ca<sup>2+</sup>-binding sites (15).

## Ca<sup>2+</sup> association and dissociation

We have modeled Ca<sup>2+</sup> binding to each EF hand pair in CaM according to a sequential model, as illustrated by Scheme 1. By convention, the two Ca<sup>2+</sup>-binding steps corresponding with occupancy of the C-ter EF hand pair are numbered 1 and 2 (as in Scheme 1), while the two N-ter Ca<sup>2+</sup>-binding steps are numbered 3 and 4. A sequential Ca<sup>2+</sup> binding model is the simplest one that accounts for the fact that dissociation of both Ca<sup>2+</sup> ions from an EF hand pair is always observed to occur with a single apparent rate (19,20). The trivial explanation that Ca<sup>2+</sup> dissociates independently from both sites at the same rate is inconsistent with the high degree of binding cooperativity (19). It is also inconsistent with <sup>15</sup>N spin relaxation experiments, which indicate that the second Ca<sup>2+</sup> release step is at least 100 times faster than the first (21). Since the second Ca<sup>2+</sup> ion is released much faster than the first, we also treat the first Ca<sup>2+</sup> binding step as rapidly equilibrating. This assumption becomes invalid at free Ca<sup>2+</sup> concentrations where  $k_2[\text{Ca}^{2+}] \approx k_{-1}$  or  $k_4[\text{Ca}^{2+}] \approx k_{-3}$ , but it appears to be applicable over the range of Ca<sup>2+</sup> concentrations used in these investigations (see Fig. 5).

## The transition from Ca<sup>2+</sup>-saturated to Ca<sup>2+</sup>-free complex

The data presented in Fig. 4 were globally fit to the kinetic model given in scheme 2. In this scheme, B corresponds with BSCaM<sub>IQ</sub>, NC corresponds with Ca<sup>2+</sup>-free CaM, and N<sub>2</sub>C<sub>2</sub> corresponds with CaM in which both the N-ter (N) and C-ter (C) EF hand pairs are replete with Ca<sup>2+</sup>. Intermediate Ca<sup>2+</sup>-bound states are designated appropriately. Since Ca<sup>2+</sup> dissociates much more rapidly from the N-ter EF hand pair than it does from the C-ter pair, dissociation of Ca<sup>2+</sup> is treated as a sequential process, with the N-ter pair of sites going first. The vertical dashed arrows denote steps that were omitted from fitting calculations because dissociation of the second Ca<sup>2+</sup> ion from an EF hand pair is assumed to be much faster than dissociates of BSCaM<sub>IQ</sub>. “Fast” rate constants were arbitrarily assigned values 10-fold larger than the rate constants preceding them.

## Release of BSCaM<sub>IQ</sub> after addition of Ca<sup>2+</sup> and ckPEP

The data presented in Fig. 5 were globally fit according to the model given in Scheme 3. In this scheme, P corresponds with a peptide (ckPEP) based on the CaM-binding domain in CaM kinase II. Since the peptide prevents reassociation of CaM, rate constants for reversal of the second C-ter Ca<sup>2+</sup>-binding step ( $k_{-2}$  and  $k'_{-2}$ ) can be omitted because the rate constants for dissociation of the CaM complex ( $k - NC_2$  and  $k_{N_2C_2}^T$ ) are much larger (see Table 1 and Table 2). Dissociation of the Ca<sup>2+</sup>-free complex can also be ignored, as it occurs at a rate of  $\sim 1 \text{ s}^{-1}$ , which is far slower than the Ca<sup>2+</sup> binding steps. Dissociation of CaM from other intermediates

is effectively irreversible due the presence of a large molar excess of ckPEP. Since the dissociation rate constant for the  $N_2C$ -B complex ( $k_{N_2C}$ ) is much smaller than  $k'_{-4}$  (see Table 1 and Table 2), we can treat both N-ter  $Ca^{2+}$ -binding steps on the lower pathway in the scheme as rapidly equilibrating, with dissociation constants of  $K'_3, K'_4$ . This approach is not applicable to the N-ter  $Ca^{2+}$ -binding steps on the upper pathway because the apparent  $Ca^{2+}$  dissociation rate constant for the N-ter sites ( $k_{-4}$ ) is similar to the rate for dissociation of a presumptive peptide ternary complex ( $k_{N_2C}^T$ ; see Table 1 and Table 2). However, this is not a significant issue because the bracketed steps can be omitted from fitting calculations without significantly affecting the fit or the derived parameter values. The probable basis for this is explained under "Results".

## Results

### Association of CaM and BSCaM<sub>IQ</sub>

The first step in these investigations was to derive apparent association and dissociation rate constants ( $k_{on}$  and  $k_{off}$ ) for the various complexes between native or mutant CaM and BSCaM<sub>IQ</sub>, a fluorescent reporter containing the IQ domain from neuromodulin (15). This was accomplished by determining observed association rates ( $k_{obs}$ ) under pseudo-first order conditions at a series of different CaM concentrations. Values for  $k_{on}$  and  $k_{off}$  were then derived from linear least-squares fits to replots of  $k_{obs}$  vs [CaM]. Values for  $k_{on}$  and  $k_{off}$  of  $3.6 \pm 0.2 \times 10^5 \text{ M}^{-1}\text{s}^{-1}$  and  $0.9 \pm 0.2 \text{ s}^{-1}$  were derived for the  $Ca^{2+}$ -free native CaM complex from the replot presented in Fig. 1A. The  $k_{off}/k_{on}$  ratio of  $2.5 \pm 0.6 \mu\text{M}$  calculated for this complex is essentially identical to the equilibrium  $K_d$  value of  $2.3 \pm 0.1 \mu\text{M}$  (Table 1). Similar rate constants were derived for the  $Ca^{2+}$ -free  $N_x$ CCaM and  $NC_x$ CaM complexes (Table 1; data not shown). Values for  $k_{on}$  and  $k_{off}$  of  $1.1 \pm 0.2 \times 10^6 \text{ M}^{-1}\text{s}^{-1}$  and  $30.9 \pm 1.6 \text{ s}^{-1}$  were derived for the  $Ca^{2+}$ -saturated  $NC_x$ CaM complex from the replot in Fig. 1B, and the  $k_{off}/k_{on}$  ratio of  $28.1 \pm 5.3 \mu\text{M}$  calculated for this complex agrees well with the equilibrium  $K_d$  value of  $36.7 \pm 3.9 \mu\text{M}$  (Table 1). Values for  $k_{on}$  and  $k_{off}$  of  $3.1 \pm 0.2 \times 10^7 \text{ M}^{-1}\text{s}^{-1}$  and  $69.4 \pm 9.6 \text{ s}^{-1}$  were derived for the  $Ca^{2+}$ -saturated complex with native CaM from the replot in Fig. 1C; and respective values of  $4.1 \pm 0.2 \times 10^7 \text{ M}^{-1}\text{s}^{-1}$  and  $558.8 \pm 10.1 \text{ s}^{-1}$  were derived for the  $Ca^{2+}$ -saturated  $N_x$ CCaM complex from the replot in Fig. 1D. The  $k_{off}/k_{on}$  ratios of  $2.2 \pm 0.3$  and  $13.6 \pm 1.1 \mu\text{M}$  calculated for these complexes are essentially identical to their equilibrium  $K_d$  values of  $2.5 \pm 0.1$  and  $14.4 \pm 1.3 \mu\text{M}$  (Table 1). The overall agreement between  $k_{off}/k_{on}$  ratios and equilibrium  $K_d$  values confirms that CaM binding to the neuromodulin IQ domain is a simple bimolecular process. Occupancy of one or both EF hand pairs in CaM significantly accelerates binding kinetics, although the greatest effect is seen when the C-ter EF hand pair is occupied. The accelerated rates observed in the presence of  $Ca^{2+}$  may serve to mobilize neuromodulin-bound CaM in response to a  $Ca^{2+}$  signal. The association rate constants for the CaM-IQ domain complexes in which the C-ter EF hand pair is  $Ca^{2+}$  bound are similar to those for the complexes between CaM and canonical target proteins, such as myosin light chain kinase or nitric oxide synthase (22,23). In contrast, the association rates derived for complexes in which the C-ter EF hand pair is  $Ca^{2+}$ -free are 30–100 times slower.

### Dissociation of CaM in the presence of CaM-binding peptides

We extended our analysis of the kinetics of native and mutant CaM-BSCaM<sub>IQ</sub> complexes by examining dissociation in the presence of a large molar excess of peptides based on the IQ domain in neurogranin (ngPEP) and the CaM-binding domain in CaM kinase II (ckPEP), which does not bind CaM with significant affinity in the absence of  $Ca^{2+}$ . In the presence of ngPEP,  $Ca^{2+}$ -free native CaM dissociates with an apparent rate constant of  $0.8 \pm 0.2 \text{ s}^{-1}$  (Fig. 2A), and essentially identical rate constants were derived for the  $Ca^{2+}$ -free complexes with the two mutant CaMs (data not shown). In the presence of ckPEP,  $Ca^{2+}$ -saturated  $NC_x$ CaM and  $N_x$ CCaM dissociate with rate constants of  $30.2 \pm 4.2$  and  $630.7 \pm 16.4 \text{ s}^{-1}$  (Figs. 2B and D). These

values agree with those derived from replots of  $k_{obs}$  vs [CaM] (Table 1). In contrast,  $\text{Ca}^{2+}$ -saturated native CaM dissociates with an apparent rate constant of  $565.1 \pm 13.1 \text{ s}^{-1}$  in the presence of ckPEP (Fig. 2C), which is  $\sim 10$ -fold faster than the rate derived from a replot of  $k_{obs}$  vs [CaM] (Table 1). The accelerated dissociation rate observed in the presence of ckPEP indicates that dissociation occurs via a ternary complex between ckPEP, CaM and BSCaM<sub>IQ</sub>. Since the measured fluorescence time course is monophasic and has an amplitude consistent with formation of free BSCaM<sub>IQ</sub>, formation of the ternary complex itself does not appear to be associated with a significant change in fluorescence. However, it is conceivable that the fluorescence time course corresponds with formation of the ternary complex itself, rather than dissociation of BSCaM<sub>IQ</sub>. This is unlikely because the apparent dissociation rate does not exhibit a second-order dependence on the ckPEP concentration (data not shown).

### Dissociation of $\text{Ca}^{2+}$

We have previously reported that under equilibrium conditions  $\text{Ca}^{2+}$  binding to the C-ter EF hand pair in the CaM-BSCaM<sub>IQ</sub> complex reduces the affinity of the complex, and subsequent binding to the N-ter EF hand pair raises it (15). The  $\text{Ca}^{2+}$ -binding affinity of the C-ter EF hand pair is thus reduced due to negative energy coupling, while the affinity of the N-ter pair is increased due to positive energy coupling (15). To investigate the mechanistic basis for these changes in  $\text{Ca}^{2+}$ -binding affinity, we determined  $\text{Ca}^{2+}$  dissociation rates for free and bound native and mutant CaMs. In general agreement with others (19,24–27),  $\text{Ca}^{2+}$  was found to dissociate from the C-ter and N-ter EF hand pairs in free CaM with rate constants of  $10.3 \pm 0.7$  and  $1152 \pm 117 \text{ s}^{-1}$ . It is important to note that dissociation rate constants were determined for free CaM using a 5  $\mu\text{l}$  observation cell, rather than the standard 20  $\mu\text{l}$  cell. This reduces the dead time of the stopped-flow fluorometer to below 1 ms, allowing this fast rate to be measured. Unfortunately, efficient rapid mixing was not obtained when we attempted to use the smaller cell with solutions containing BSCaM<sub>IQ</sub>, presumably due to their higher viscosities. Dissociation rate constants of  $11.7 \pm 0.5 \text{ s}^{-1}$  and  $473.4 \pm 37.9 \text{ s}^{-1}$  were derived when CaM is bound to BSCaM<sub>IQ</sub> (Fig. 3A). To confirm that the slower rate constant corresponds with the C-ter EF hand pair, dissociation rate constants were derived for N<sub>x</sub>CCaM in the presence and absence of BSCaM<sub>IQ</sub> (Fig. 3B), and respective values of  $11.8 \pm 0.5$  and  $10.8 \pm 0.6 \text{ s}^{-1}$  were obtained. The dissociation rate constant of  $473.4 \pm 37.9 \text{ s}^{-1}$  derived for the native CaM complex therefore corresponds with the N-ter EF hand pair and the slower rate corresponds with the C-ter pair. The increased  $\text{Ca}^{2+}$ -binding affinity of the N-ter sites in the CaM-BSCaM<sub>IQ</sub> complex is thus correlated with a decrease in the dissociation rate for  $\text{Ca}^{2+}$ . The reduced affinity of the C-ter pair of sites does not appear to involve a change in the  $\text{Ca}^{2+}$  dissociation rate. Determination of a  $\text{Ca}^{2+}$  dissociation rate for the NC<sub>x</sub>CaM-BSCaM<sub>IQ</sub> complex, which exhibits negative energy coupling (15), was not possible because maintenance of the complex requires BSCaM<sub>IQ</sub> solutions with viscosities that preclude efficient mixing.

### The transition from $\text{Ca}^{2+}$ -saturated to $\text{Ca}^{2+}$ -free complex

Having determined binding kinetics and  $\text{Ca}^{2+}$  dissociation rates for mutant and native CaM-BSCaM<sub>IQ</sub> complexes, we next analyzed the fluorescence changes associated with the transition from the  $\text{Ca}^{2+}$ -saturated to the  $\text{Ca}^{2+}$ -free complex. Fluorescence time courses were measured after addition of a large molar excess of BAPTA to the  $\text{Ca}^{2+}$ -saturated CaM-BSCaM<sub>IQ</sub> complex (Fig. 4A and B). Individual time courses measured on different time scales are offset in the figure for presentation purposes. These data were globally fit to the kinetic model presented in Scheme 2. In this model  $\text{Ca}^{2+}$ -dissociates sequentially from the N-ter and C-ter EF hand pairs because the N-ter sites have much faster kinetics. Relative molar fluorescence amplitudes were assigned to all kinetic species as detailed under “Materials and Methods”. The fitted curves presented in the figure were generated by varying only  $k'_{-2}$  and  $k'_{-4}$ , the  $\text{Ca}^{2+}$  dissociation rate constants for N-ter and C-ter EF hand pairs in bound CaM. All other necessary parameters were fixed to the values given in Table 1 & Table 2. Parameter values derived for

$N_xCCaM$  were applied to the intermediate species in which  $Ca^{2+}$  remains bound to the C-ter EF hand pair ( $NC_2-B$ ). Rate constants for “fast” steps were arbitrarily assigned values 10-fold higher than the rate constants for the steps preceding them. The rising phase in fluorescence corresponds largely with formation and dissociation of the  $NC_2-B$  intermediate, although dissociation of the initial  $Ca^{2+}$ -saturated complex due to dilution also contributes. The falling phase corresponds with formation of the final  $Ca^{2+}$ -free complex, which is not as fluorescent as the initial complex. The slight discrepancy between the fitted curves and the data measured during the first few milliseconds is probably due to the simplifying assumption that short-lived intermediates with  $Ca^{2+}$  bound to only a single site in an EF hand pair are effectively non-dissociating (dashed arrows in Scheme 2). The overall quality of the fit suggests that this scheme nevertheless represents a reasonable minimal model. The validity of the model is lent further support by the fact that fitted values of  $13.5 \pm 0.1$  and  $528.3 \pm 3.3$   $s^{-1}$  were derived for  $k'_{-2}$  and  $k'_{-4}$ , which are essentially identical to the  $Ca^{2+}$ -dissociation rate constants derived from  $Ca^{2+}$  trapping experiments (Table 2).

### $Ca^{2+}$ -dependent release of CaM in the presence of a CaM-binding peptide

Given the hypothesis that neuromodulin participates in CaM storage and delivery (9,28,29), we were particularly interested in investigating release of CaM from the neuromodulin IQ domain in the presence of  $Ca^{2+}$  and a peptide (ckPEP) based on the CaM-binding domain in CaM kinase II, an abundant enzyme in neurons (30). From an experimental standpoint, analysis of this process is complicated by the fact that two pathways for sequential occupancy of the N-ter and C-ter EF hand pairs must be considered (see Scheme 3). We therefore initially analyzed the behavior of the  $N_xCCaM-BSCaMIQ$  complex to eliminate the contribution of the N-ter pair of  $Ca^{2+}$  binding sites.

Fluorescence time courses measured after adding excess ckPEP and different amounts of  $Ca^{2+}$  to the  $Ca^{2+}$ -free mutant complex are presented in Fig. 5A. These data were globally fit according to the steps in Scheme 3 that correspond with formation and dissociation of the intermediate  $NC_2-B$  complex. The second  $Ca^{2+}$ -binding step is effectively irreversible because  $Ca^{2+}$  dissociates from the  $NC_2-B$  complex at a rate of  $\sim 10$   $s^{-1}$ , while the complex itself dissociates at a rate of  $\sim 500$   $s^{-1}$  (Table 1 & Table 2). The fit presented in Panel A was produced by varying the dissociation constant ( $K_I$ ) for the first C-ter  $Ca^{2+}$ -binding step and the association rate constant ( $k_2$ ) for the second  $Ca^{2+}$ -binding step. The other necessary parameter was the dissociation rate constant for the  $NC_2-B$  intermediate ( $k-NC_2$ ), which was fixed to the value given in Table 2. Dissociation of this intermediate is effectively irreversible, as there is a large molar excess of ckPEP. Relative molar fluorescence amplitudes were assigned to all kinetic species as detailed under “Materials and Methods”. The observed increases in fluorescence reflect the increase that occurs when the  $NC_2-B$  intermediate forms, and the further increase that occurs when it dissociates. The quality of the fit suggests that a three step kinetic model we have used is a reasonable minimal description of this process. The fitted values obtained for  $K_I$  and  $k_2$  are  $4.8 \pm 0.9$   $\mu M$  and  $3.1 \pm 0.1 \times 10^6$   $M^{-1} \cdot s^{-1}$ . The latter value is  $\sim 10$ -fold less than the  $Ca^{2+}$  association rate constant estimated for free CaM (Table 2).

We next measured a series of fluorescence time courses for the native  $CaM-BSCaMIQ$  complex using the same experimental approach (Fig. 5B). These data were globally fit according to the model depicted in Scheme 3. The rate constant for dissociation of the  $Ca^{2+}$  saturated  $CaM-BSCaMIQ$  complex in the presence of ckPEP is designated as  $k_{N_2C_2}^T$ , since this step appears to involve formation of a ternary complex with the peptide. The bracketed portion of the scheme can be omitted from fitting calculation without significant effect, apparently because in the presence of ckPEP the  $NC_2-B$  and  $N_2C_2-B$  intermediates dissociate at essentially the same rate (Table 2), and there is also little difference in their fluorescence (15). Binding of  $Ca^{2+}$  to the N-ter EF hand pair prior to the C-ter pair is modeled as rapidly equilibrating because the rates

at which  $N_2C-B$  dissociates or is converted to the  $N_2C_2-B$  intermediate are relatively slow (see Table 1 and Table 2). The fit shown in Fig. 5B was produced by varying only  $K'_1$  and  $k'_2$ . Previously-determined dissociation constants of 122 and 9.4  $\mu\text{M}$  were assigned to  $K'_3$  and  $K'_4$  (15). Other required kinetic parameters, including  $K_1$  and  $k_2$ , were fixed to the values given in Table 1 & Table 2. The parameters for reactions involving  $NC_2-B$  and  $N_2C-B$  were derived using  $N_xCCaM$  and  $NC_xCaM$ . Relative molar fluorescence amplitudes were assigned to all kinetic species as detailed under "Materials and Methods". The observed fluorescence time courses reflect increases due to formation of the  $NC_2-B$  and  $N_2C-B$  intermediates, and to release of  $BSCaM_{IQ}$  (B). Formation of the  $N_2C-B$  intermediate produces a fluorescence increase that occurs within the  $\sim 1.4$  ms dead time of the stopped-flow (Fig. 5B). This increase thus corresponds with rapidly-equilibrating binding of  $Ca^{2+}$  to the N-ter EF hand pair, and its amplitude increases as a function of the free  $Ca^{2+}$  concentration in accordance with the values used for  $K'_3$  and  $K'_4$ . The amplitude of this phase is also linked to the amount of  $BSCaM_{IQ}$  dissociation occurring via the lower pathway in Scheme 3. Thus, at a free  $Ca^{2+}$  concentration of  $\sim 10$   $\mu\text{M}$ , dissociation via this pathway is negligible, while at a free  $Ca^{2+}$  concentration of  $\sim 70$   $\mu\text{M}$  dissociation via the upper and lower pathways is equivalent (data not shown). At a free  $Ca^{2+}$  concentration of 250  $\mu\text{M}$  the proportion of dissociation via the lower pathway saturates at a value of  $\sim 65\%$ . This occurs in spite of the much faster  $Ca^{2+}$ -binding kinetics of the N-ter EF hand pair because the  $N_2C-B$  intermediate dissociates relatively slowly. The overall quality of the fit indicates that Scheme 3 represents an acceptable minimal kinetic model. Fitted values of  $4.1 \pm 0.6$   $\mu\text{M}$  and  $3.2 \pm 0.1 \times 10^6$   $\text{M}^{-1}\text{s}^{-1}$  were derived for  $K'_1$  and  $k'_2$ , which are not significantly different from the values derived for  $K_1$  and  $k_2$ . The association rate constant for the C-ter  $Ca^{2+}$ -binding sites in CaM therefore appears to be reduced to the same extent, regardless of whether  $Ca^{2+}$  is bound to the N-ter pair of sites.

## Discussion

In this paper we present the results of a kinetic analysis of the complex between CaM and  $BSCaM_{IQ}$ , a fluorescent reporter containing the IQ domain from neuromodulin (15). Association and dissociation rate constants for various  $Ca^{2+}$ -bound forms of the complex were determined, as well as many of the rate constants governing  $Ca^{2+}$  binding to the complex. Kinetic models incorporating these rate constants were developed that account for the  $BSCaM_{IQ}$  fluorescence responses observed when  $Ca^{2+}$  is removed from the  $Ca^{2+}$ -saturated complex or when  $Ca^{2+}$  is added to the  $Ca^{2+}$ -free complex in the presence of a peptide based on the CaM-binding domain in CaM kinase II. Three key points are evident: (1) Association and dissociation of the complex is accelerated in the presence of  $Ca^{2+}$ . (2) When CaM is bound to the IQ domain, the  $Ca^{2+}$ -association rate constant for the C-ter EF hand pair is reduced  $\sim 10$ -fold and the  $Ca^{2+}$ -dissociation rate constant for the N-ter EF hand pair is reduced  $\sim 3$ -fold. (3)  $Ca^{2+}$ -saturated CaM can be transferred from the neuromodulin IQ domain to canonical CaM-binding domains, such as the one in CaM kinase II, via an intermediate ternary complex.

### CaM-binding kinetics

As seen in Table 1, there is complete agreement between the association and dissociation rate constants for various native and mutant CaM- $BSCaM_{IQ}$  complexes derived from replots of  $k_{\text{obs}}$  vs  $[\text{CaM}]$  and the corresponding equilibrium  $K_d$  values. The association and dissociation rates for the  $Ca^{2+}$ -saturated CaM-IQ domain complex and the C-ter  $Ca^{2+}$ -bound intermediate are 30 to 100-fold faster than for the  $Ca^{2+}$ -free complex (Table 1). The association rate constants derived for the  $Ca^{2+}$ -saturated complex and the C-ter  $Ca^{2+}$ -bound intermediate are similar to those derived for the  $Ca^{2+}$ -saturated complexes between CaM and other types of CaM-binding sequences (22,23,31). The kinetics of the N-ter  $Ca^{2+}$ -bound intermediate are comparatively slow, as its association rate constant is only 3-fold faster than the rate constant

for the  $\text{Ca}^{2+}$ -free complex (Table 1). This indicates that slow binding kinetics are a feature of interactions between the  $\text{Ca}^{2+}$ -free C-ter CaM lobe and the IQ domain.

Dissociation rate constants were also determined for native and mutant CaM-BSCaM<sub>IQ</sub> complexes by using ckPEP or ngPEP to trap CaM. With only one exception, these values agree with those derived from replots of  $k_{obs}$  vs [CaM] (Table 1). The exception is the  $\text{Ca}^{2+}$ -saturated native CaM-BSCaM<sub>IQ</sub> complex, which dissociates at a rate of  $565.1 \pm 13.1$  in the presence of ckPEP, compared with a rate of  $69.4 \pm 9.6$  derived from an analysis of binding kinetics (Table 1). Dissociation is accelerated in the presence of the peptide, since the slower rate is consistent with the  $K_d$  value for this complex (Table 1). The only reasonable explanation for this behavior is that in the presence of ckPEP dissociation occurs via a ternary complex between the peptide, CaM and BSCaM<sub>IQ</sub>. The absence of an effect of ckPEP on the dissociation rates for the intermediate CaM-BSCaM<sub>IQ</sub> complexes in which  $\text{Ca}^{2+}$  is bound only to the N-ter or C-ter EF hand pair suggests that neither can participate in a ternary complex, or that they do so with no apparent effect on their kinetic properties. Gaertner and co-workers have previously presented evidence consistent with formation of a ternary complex between intact CaM kinase II, CaM and the IQ domain in neurogranin (32). A ternary complex intermediate provides a route for efficient delivery of CaM from neuromodulin to other CaM-binding proteins, consistent with its proposed role in CaM storage and delivery.

### Ca<sup>2+</sup>-binding kinetics

$\text{Ca}^{2+}$  dissociation rates for the N-ter and C-ter EF hand pairs in bound native and mutant CaMs were directly evaluated in  $\text{Ca}^{2+}$  trapping experiments (Table 2). These rates agree with those derived from a global analysis BSCaM<sub>IQ</sub> fluorescence data measured during the transition from the  $\text{Ca}^{2+}$ -saturated to the  $\text{Ca}^{2+}$ -free complex (Fig. 4A and B; Table 2). The dissociation rate derived for the N-ter EF hand pair in bound CaM ( $k'_{-4}$ ) is  $473.4 \pm 37.9 \text{ s}^{-1}$ , while the corresponding value for free CaM ( $k_{-4}$ ) is  $1298 \pm 135 \text{ s}^{-1}$ . In principle, the  $k_{-4}/k'_{-4}$  ratio of  $2.7 \pm 0.4$  should be comparable to the  $K_4/K'_4$  ratio, but in practice the individual dissociation constants for an EF hand pair are not as well determined as the product of the constants (15). It is therefore preferable to compare the  $K_3K_4/K'_3K'_4$  ratio with the square of the  $k_{-4}/k'_{-4}$  ratio. The latter ratio is squared because  $k_{-4}$  and  $k'_{-4}$  both correspond with dissociation of two  $\text{Ca}^{2+}$  ions (see Scheme 2). The value of  $10.2 \pm 1.8$  derived for  $K_3K_4/K'_3K'_4$  from data published previously is in reasonable agreement with the square of  $k_{-4}/k'_{-4}$ , which is  $7.3 \pm 1.1$  (15). This suggests that the increased  $\text{Ca}^{2+}$ -binding affinity of the N-ter EF hand pair in the CaM-IQ domain complex is due to a decreased  $\text{Ca}^{2+}$  dissociation rate. The  $\text{Ca}^{2+}$  dissociation rates determined for the C-ter EF hand pair in bound and free CaM are essentially identical (Table 2), so the reduced affinity of these sites in the CaM-IQ domain complex is not due to an accelerated dissociation rate.

Association rates for  $\text{Ca}^{2+}$  were derived for the C-ter EF hand pair in bound CaM from a global analysis of fluorescence data measured after addition of  $\text{Ca}^{2+}$  and ckPEP to the  $\text{Ca}^{2+}$ -free native or  $\text{N}_x\text{CCaM}$  complex with BSCaM<sub>IQ</sub> (Fig. 5A and B; Table 2). Association rates could not be determined for the N-ter EF hand pair. Since essentially the same kinetic parameters were derived for the C-ter EF hand pairs in the native and  $\text{N}_x\text{CCaM}$  complexes with BSCaM<sub>IQ</sub>, we shall only discuss our analysis of the latter in detail. We have modeled  $\text{Ca}^{2+}$  binding to an EF hand pair as a sequential process, with a rapidly equilibrating first step and a slower second step. Fitted values of  $4.6 \pm 0.9 \text{ }\mu\text{M}$  and  $3.1 \pm 0.1 \times 10^6 \text{ M}^{-1}\text{s}^{-1}$  were derived for  $K_1$ , the dissociation constant for the first step and  $k_2$ , the association rate constant for the second step. In the presence of ckPEP, we can ignore  $k_{-2}$ , the rate constant for reversal of the second step, because  $\text{Ca}^{2+}$  dissociates ~50-fold slower from the complex than does  $\text{Ca}^{2+}$ -saturated  $\text{N}_x\text{CCaM}$ , which is then trapped by ckPEP (Table 1). The value derived for  $k_2$  is ~10-fold less than the corresponding value for free  $\text{N}_x\text{CCaM}$  (Table 2). By combining the values we have



derived for  $K_1$  and  $k_2$  with a  $k_{-2}$  value of  $11.8 \pm 0.5$  (Table 2), we can calculate a value of  $18.2 \pm 5.1 \mu\text{M}^2$  for the product of the two  $\text{Ca}^{2+}$  dissociation constants for the  $\text{N}_x\text{CCaM-BSCaMIQ}$  complex. This is in reasonable agreement with the value of  $24.6 \pm 2.7 \mu\text{M}^2$  derived from equilibrium  $\text{Ca}^{2+}$ -binding data (15). Thus, the reduced affinity of the C-ter EF hand pair in bound CaM appears to be due to a reduced  $\text{Ca}^{2+}$  association rate, as expected given the absence of any effect on the dissociation rate.

A surprising aspect of our results is that the same association rate constant is derived for  $\text{Ca}^{2+}$  binding to the C-ter EF hand pair, regardless of whether the N-ter EF hand pair is occupied by  $\text{Ca}^{2+}$ . Since the affinity of C-ter EF hand pair for  $\text{Ca}^{2+}$  is higher when the N-ter sites are occupied, it appears that the dissociation rate constant must be reduced to account for this (15). This is difficult to prove because  $\text{Ca}^{2+}$  dissociates from the C-ter sites much more slowly than it does from the N-ter sites. Thus, dissociation from the C-ter sites while the N-ter sites remain occupied cannot be observed in  $\text{Ca}^{2+}$  trapping experiments.

### Implications for neuromodulin function

We have shown previously that under equilibrium conditions the apparent dissociation constant for the neuromodulin CaM-IQ domain complex has a bell-shaped dependence on the free  $\text{Ca}^{2+}$  concentration, peaking at a concentration of  $\sim 6 \mu\text{M}$  (15). Thus, release of CaM is promoted over a relatively narrow range of free  $\text{Ca}^{2+}$  concentrations. During a  $\text{Ca}^{2+}$  transient in a neuron the free  $\text{Ca}^{2+}$  concentration is likely to pass rapidly through this range, so we have proposed that release of CaM is only promoted briefly (15). Although the bell-shaped response curve has important implications with regard to regulation via CaM-IQ domain switches under equilibrium or quasi-equilibrium conditions, the analysis presented in this paper suggests some modifications to our understanding of what occurs during a rapid  $\text{Ca}^{2+}$  transient. The overall picture that emerges is one in which neuromodulin continuously maintains a local store of CaM that is efficiently delivered to target proteins in its  $\text{Ca}^{2+}$ -bound form during a  $\text{Ca}^{2+}$  transient.

The principal difference between the equilibrium and transient behaviors of the CaM-IQ domain complex is that the N-ter  $\text{Ca}^{2+}$ -bound intermediate plays a significant role when  $\text{Ca}^{2+}$  is rapidly increased to levels above  $10 \mu\text{M}$ , as can occur locally during a neuronal  $\text{Ca}^{2+}$  transient (33–38). This intermediate does not form to a significant extent under equilibrium conditions, primarily because the C-ter  $\text{Ca}^{2+}$ -binding sites, although slower kinetically, have an  $\text{EC}_{50}(\text{Ca}^{2+})$  of  $\sim 5 \mu\text{M}$ , while the value for the N-ter sites is  $\sim 35 \mu\text{M}$  (15). The N-ter  $\text{Ca}^{2+}$  bound intermediate dissociates at a relatively slow rate of  $\sim 30 \text{ s}^{-1}$ , compared with a rate of  $\sim 500 \text{ s}^{-1}$  for the C-ter intermediate. The kinetic properties of the CaM-IQ domain complex therefore appear to inhibit release of CaM in its  $\text{Ca}^{2+}$  free and N-ter  $\text{Ca}^{2+}$  bound intermediate forms (Table 1). When the C-ter  $\text{Ca}^{2+}$ -bound CaM intermediate dissociates it is presumably captured by target proteins and rapidly converted to  $\text{Ca}^{2+}$ -saturated CaM, given the essentially diffusion-limited  $\text{Ca}^{2+}$  association rate constants for the N-ter EF hand pair (Table 2). If the N-ter  $\text{Ca}^{2+}$ -bound intermediate were to dissociate to a significant extent it could have negative consequences. First, since at least some targets appear to capture CaM via its C-ter lobe, the N-ter  $\text{Ca}^{2+}$ -bound intermediate may simply not be bound in some cases (39). Second, if a target were to capture this intermediate, the relatively slow  $\text{Ca}^{2+}$  association rate constants for the C-ter EF hand pair could impose a significant delay on target activation (Table 2). An implication of the latter point is that an abundant localized store accelerates production of CaM in its  $\text{Ca}^{2+}$ -saturated and C-ter  $\text{Ca}^{2+}$ -bound intermediate forms sufficiently to meet the speed requirements of neuronal signaling. Given a high enough local CaM concentration, this could be effected through simple mass action. The similar affinities of neuromodulin for  $\text{Ca}^{2+}$ -free and  $\text{Ca}^{2+}$ -saturated CaM may serve not only to minimize diffusional losses of CaM, as we have proposed previously, but also to continuously replenish the CaM store through diffusional recruitment from adjacent regions in the cell. The degree to which ternary complexes play a

role in CaM delivery in neurons remains to be established, although they clearly have the potential to facilitate this process.

We are currently extending these investigations by determining how the CaM-IQ domain complex responds to synthetic Ca<sup>2+</sup> transients. In conjunction with extensive modeling, this approach should allow us to develop a more quantitative understanding of Ca<sup>2+</sup> switching among various states. The kinetic aspects of the CaM-IQ domain complex that we have described are likely to have counterparts in systems that are functionally modulated by CaM-IQ domain switches, such as ion channels and unconventional myosins. A particular intriguing possibility is that ratio of the N-ter and C-ter Ca<sup>2+</sup>-bound intermediates that is produced during a Ca<sup>2+</sup> transient provides a mechanism for producing functional responses that depend upon the amplitude and speed of the transient.

## References

1. Yagi K, Yazawa M, Kakiuchi S, Ohshima M, Uenishi K. Identification of an activator protein for myosin light chain kinase as the Ca<sup>2+</sup>-dependent modulator protein. *J. Biol. Chem* 1978;253:1338–1340. [PubMed: 627540]
2. Bredt DS, Snyder SH. Isolation of nitric oxide synthetase, a calmodulin-requiring enzyme. *Proc. Nat. Acad. Sci. U.S.A* 1990;87:682–685.
3. Venema RC, Sayegh HS, Arnal JF, Harrison DG. Role of the enzyme calmodulin-binding domain in membrane association and phospholipid inhibition of endothelial nitric oxide synthase. *J. Biol. Chem* 1995;270:14705–14711. [PubMed: 7540177]
4. Dabrowska R, Sherry JM, Aromatorio DK, Hartshorne DJ. Modulator protein as a component of the myosin light chain kinase from chicken gizzard. *Biochemistry* 1978;17:253–258. [PubMed: 202300]
5. Jurado LA, Chockalingam PS, Jarrett HW. Apocalmodulin. *Physiol. Rev* 1999;79:661–682. [PubMed: 10390515]
6. Bahler M, Rhoads A. Calmodulin signaling via the IQ motif. *FEBS Lett* 2002;513:107–113. [PubMed: 11911888]
7. Saimi Y, Kung C. Calmodulin as an ion channel subunit. *Annu. Rev. Physiol* 2002;64:289–311. [PubMed: 11826271]
8. Halling DB, Aracena-Parks P, Hamilton SL. Regulation of voltage-gated Ca<sup>2+</sup> channels by calmodulin. [republished from *Sci STKE*. 2005 Dec 20;2005(315):re15; PMID: 16369047]. *Science's Stke* [Electronic Resource]: *Signal Transduction Knowledge Environment* 2006;2006:er1.
9. Estep RP, Alexander KA, Storm DR. Regulation of free calmodulin levels in neurons by neuromodulin: relationship to neuronal growth and regeneration. *Curr. Top. Cell. Regul* 1990;31:161–180. [PubMed: 2147138]
10. Tran QK, Black DJ, Persechini A. Intracellular coupling via limiting calmodulin. *J. Biol. Chem* 2003;278:24247–24250. [PubMed: 12738782]
11. Rakhilin SV, Olson PA, Nishi A, Starkova NN, Fienberg AA, Nairn AC, Surmeier DJ, Greengard P. A network of control mediated by regulator of calcium/calmodulin-dependent signaling. *Science* 2004;306:698–701. [PubMed: 15499021]
12. Isotani E, Zhi G, Lau KS, Huang J, Mizuno Y, Persechini A, Geguchadze R, Kamm KE, Stull JT. Real-time evaluation of myosin light chain kinase activation in smooth muscle tissues from a transgenic calmodulin-biosensor mouse. *Proc. Natl. Acad. Sci. USA* 2004;101:6279–6284. [PubMed: 15071183]
13. Gnegy ME. Calmodulin: effects of cell stimuli and drugs on cellular activation. *Prog. Drug Res* 1995;45:33–65. [PubMed: 8545541]
14. Gerendasy DD, Herron SR, Watson JB, Sutcliffe JG. Mutational and biophysical studies suggest RC3/neurogranin regulates calmodulin availability. *J. Biol. Chem* 1994;269:22420–22426. [PubMed: 8071370]
15. Black DJ, Leonard J, Persechini A. Biphasic Ca<sup>2+</sup>-dependent switching in a calmodulin-IQ domain complex. *Biochemistry* 2006;45:6987–6995. [PubMed: 16734434]

16. Fruen BR, Black DJ, Bloomquist RA, Bardy JM, Johnson JD, Louis CF, Balog EM. Regulation of the RYR1 and RYR2 Ca<sup>2+</sup> release channel isoforms by Ca<sup>2+</sup>-insensitive mutants of calmodulin. *Biochemistry* 2003;42:2740–2747. [PubMed: 12614169]
17. Tang W, Halling DB, Black DJ, Pate P, Zhang JZ, Pedersen S, Altschuld RA, Hamilton SL. Apocalmodulin and Ca<sup>2+</sup> calmodulin-binding sites on the Ca(V)<sub>1.2</sub> channel. *Biophys. J* 2003;85:1538–1547. [PubMed: 12944271]
18. Kuzmic P. Program DYNAFIT for the analysis of enzyme kinetic data: application to HIV proteinase. *Anal. Biochem* 1996;237:260–273. [PubMed: 8660575]
19. Forsén, S.; Vogel, HJ.; Drakenberg, T. Biophysical studies of calmodulin. In: Cheung, WY., editor. *Calcium and Cell Function*. New York: Academic Press; 1986. p. 113-157.
20. Persechini A, White HD, Gansz KJ. Different Mechanisms For Ca<sup>2+</sup> Dissociation From Complexes of Calmodulin With Nitric Oxide Synthase or Myosin Light Chain Kinase. *J. Biol. Chem* 1996;271:62–67. [PubMed: 8550626]
21. Malmendal A, Evenas J, Forsen S, Akke M. Structural dynamics in the C-terminal domain of calmodulin at low calcium levels. *J. Mol. Biol* 1999;293:883–899. [PubMed: 10543974]
22. Bowman BF, Peterson JA, Stull JT. Pre-steady-state Kinetics of Activation of Rabbit Skeletal Muscle Myosin Light Chain Kinase by Ca<sup>2+</sup>/Calmodulin. *J. Biol. Chem* 1992;267:5346–5345. [PubMed: 1544916]
23. Kasturi R, Vasulka C, Johnson JD. Ca<sup>2+</sup>, caldesmon, and myosin light chain kinase exchange with calmodulin. *J. Biol. Chem* 1993;268:7958–7964. [PubMed: 8463316]
24. Bayley P, Ahlstrom P, Martin SR, Forsén S. The kinetics of calcium binding to calmodulin: Quin 2 and Ans stopped-flow fluorescence studies. *Biochem. Biophys. Res. Comm* 1984;120:185–191. [PubMed: 6712688]
25. Martin SR, Teleman AA, Bayley PM, Drakenberg T, Forsén S. Kinetics of calcium dissociation from calmodulin and its tryptic fragments. A stopped-flow fluorescence study using Quin 2 reveals a two-domain structure. *Eur. J. Biochem* 1985;151:543–550. [PubMed: 4029146]
26. Martin SR, Linse S, Bayley PM, Forsen S. Kinetics of cadmium and terbium dissociation from calmodulin and its tryptic fragments. *Eur. J. Biochem* 1986;161:595–601. [PubMed: 3792310]
27. Johnson JD, Snyder C, Walsh M, Flynn M. Effects of myosin light chain kinase and peptides on Ca<sup>2+</sup> + exchange with the N- and C-terminal Ca<sup>2+</sup> binding sites of calmodulin. *J. Biol. Chem* 1996;271:761–767. [PubMed: 8557684]
28. Chapman ER, Au D, Alexander KA, Nicolson TA, Storm DR. Characterization of the calmodulin binding domain of neuromodulin. Functional significance of serine 41 and phenylalanine 42. *J. Biol. Chem* 1991;266:207–213. [PubMed: 1824693]
29. Liu YC, Storm DR. Regulation of free calmodulin levels by neuromodulin: neuron growth and regeneration. *Trends Pharmacol. Sci* 1990;11:107–111. [PubMed: 2151780]
30. Nairn AC, Picciotto MR. Calcium/calmodulin-dependent protein kinases. *Semin. Cancer Biol* 1994;5:295–303. [PubMed: 7803766]
31. Johnson JD, Holroyde MJ, Crouch TH, Solaro RJ, Potter JD. Fluorescence studies of the interaction of calmodulin with myosin light chain kinase. *J. Biol. Chem* 1981;256:12194–12198. [PubMed: 6895374]
32. Gaertner TR, Putkey JA, Waxham MN. RC3/neurogranin and Ca<sup>2+</sup>/calmodulin-dependent protein kinase II produce opposing effects on the affinity of calmodulin for calcium. *J. Biol. Chem* 2004;279:39374–39382. [PubMed: 15262982]
33. Etter EF, Minta A, Poenie M, Fay FS. Near-membrane [Ca<sup>2+</sup>] transients resolved using the Ca<sup>2+</sup> indicator FFP18. *Proc. Natl. Acad. Sci. USA* 1996;93:5368–5373. [PubMed: 8643581]
34. Marsault R, Murgia M, Pozzan T, Rizzuto R. Domains of high Ca<sup>2+</sup> beneath the plasma membrane of living A7r5 cells. *EMBO J* 1997;16:1575–1581. [PubMed: 9130702]
35. Davies EV, Hallett MB. High micromolar Ca<sup>2+</sup> beneath the plasma membrane in stimulated neutrophils. *Biochem. Biophys. Res. Commun* 1998;248:679–683. [PubMed: 9703986]
36. Klingauf J, Neher E. Modeling Buffered Ca<sup>2+</sup> Diffusion Near the Membrane - Implications For Secretion In Neuroendocrine Cells. *Biophys. J* 1997;72:674–690. [PubMed: 9017195]
37. Simon SM, Llinas RR. Compartmentalization of the submembrane calcium activity during calcium influx and its significance in transmitter release. *Biophys. J* 1985;48:485–498. [PubMed: 2412607]

38. Llinas R, Moreno H. Local  $\text{Ca}^{2+}$  signaling in neurons. *Cell Calcium* 1998;24:359–366. [PubMed: 10091005]
39. Persechini A, McMillan K, Leakey P. Activation of myosin light chain kinase and nitric oxide synthase activities by calmodulin fragments. *J. Biol. Chem* 1994;269:16148–16154. [PubMed: 7515878]

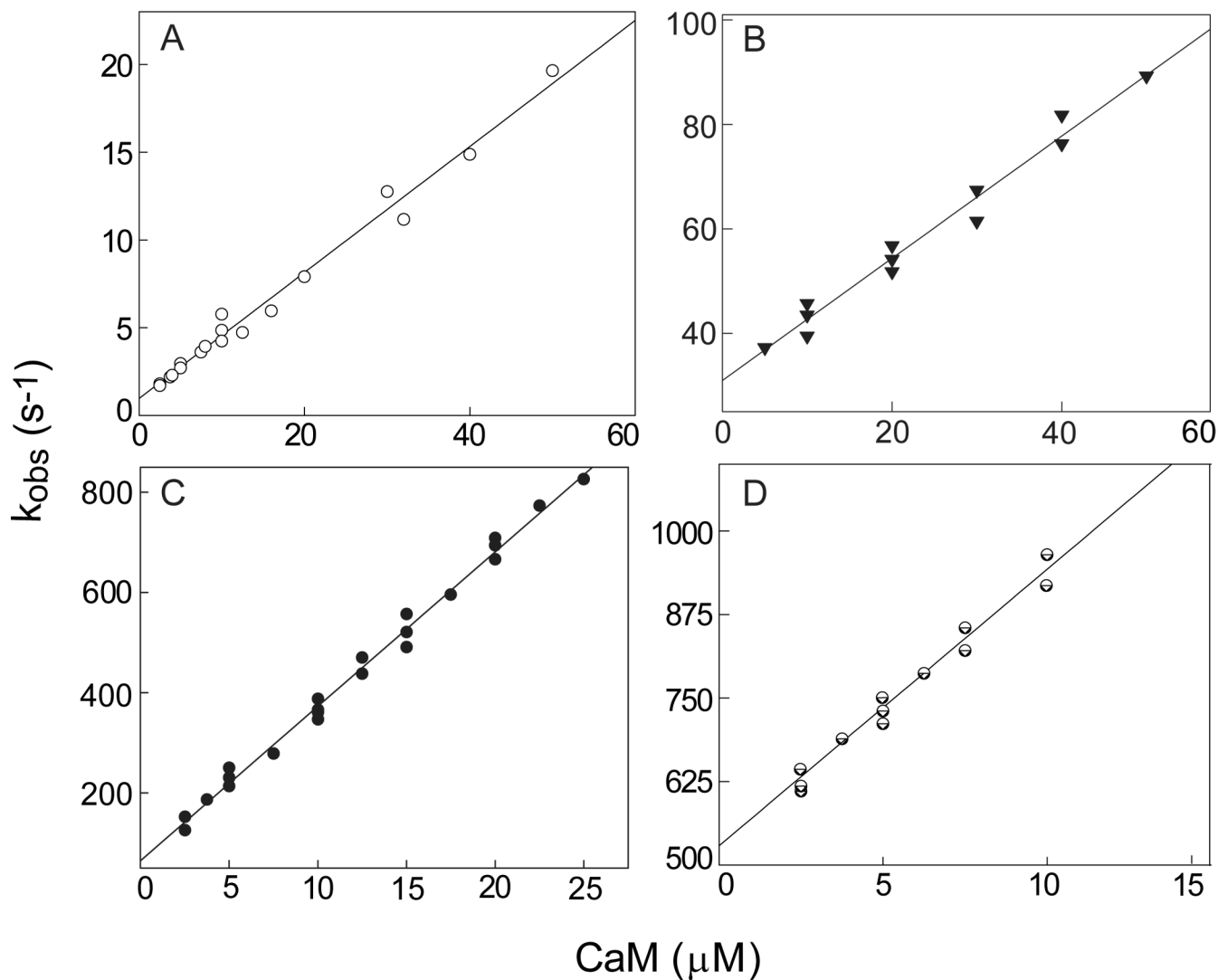


**Fig. 1. Association of native and mutant CaMs with BSCaMIQ**

Values for  $k_{obs}$  were derived from mono-exponential fits to time courses for BSCaMIQ fluorescence measured after addition of CaM. The lowest final CaM concentration produced was in all cases at least 5-fold greater than final BSCaMIQ concentration. Pseudo-first order conditions were thus maintained so that  $k_{obs} = k_{on}[CaM] + k_{off}$ . **(A)** Replot of  $k_{obs}$  values determined in the absence of  $Ca^{2+}$  vs the concentration of CaM. Nominally  $Ca^{2+}$ -free conditions were produced by including 3 mM BAPTA in all experimental buffers. The  $k_{on}$  and  $k_{off}$  values derived from the linear fit shown are  $3.6 \pm 0.2 \times 10^5 M^{-1} \cdot s^{-1}$  and  $0.9 \pm 0.2 s^{-1}$ .  $k_{on}$  and  $k_{off}$  values derived for  $Ca^{2+}$ -free  $N_xCCaM$  are  $3.2 \pm 0.1 \times 10^5 M^{-1} \cdot s^{-1}$  and  $1.1 \pm 0.1 s^{-1}$ , and values of  $2.9 \pm 0.1 \times 10^5 M^{-1} \cdot s^{-1}$  and  $0.7 \pm 0.1 s^{-1}$  were derived for  $Ca^{2+}$ -free  $NC_xCaM$  (data not shown). **(B)** Replot of  $k_{obs}$  values determined in the presence of 250  $\mu M$   $CaCl_2$  vs the concentration of  $NC_xCaM$ . The  $k_{on}$  and  $k_{off}$  values derived from the linear fit shown are  $1.1 \pm 0.2 \times 10^6 M^{-1} \cdot s^{-1}$  and  $30.9 \pm 1.6 s^{-1}$ . **(C)** Replot of  $k_{obs}$  values determined in the presence of 250  $\mu M$   $CaCl_2$  vs the concentration of native CaM. The  $k_{on}$  and  $k_{off}$  values derived from the linear fit shown are  $3.1 \pm 0.2 \times 10^7 M^{-1} \cdot s^{-1}$  and  $69.4 \pm 9.6 s^{-1}$ . **(D)** Replot of  $k_{obs}$  values determined in the presence of 250  $\mu M$   $CaCl_2$  vs the  $N_xCCaM$  concentration.  $k_{on}$  and  $k_{off}$  values of  $4.1 \pm 0.2 \times 10^7 M^{-1} \cdot s^{-1}$  and  $558.8 \pm 10.1 s^{-1}$  were derived from linear fit shown.

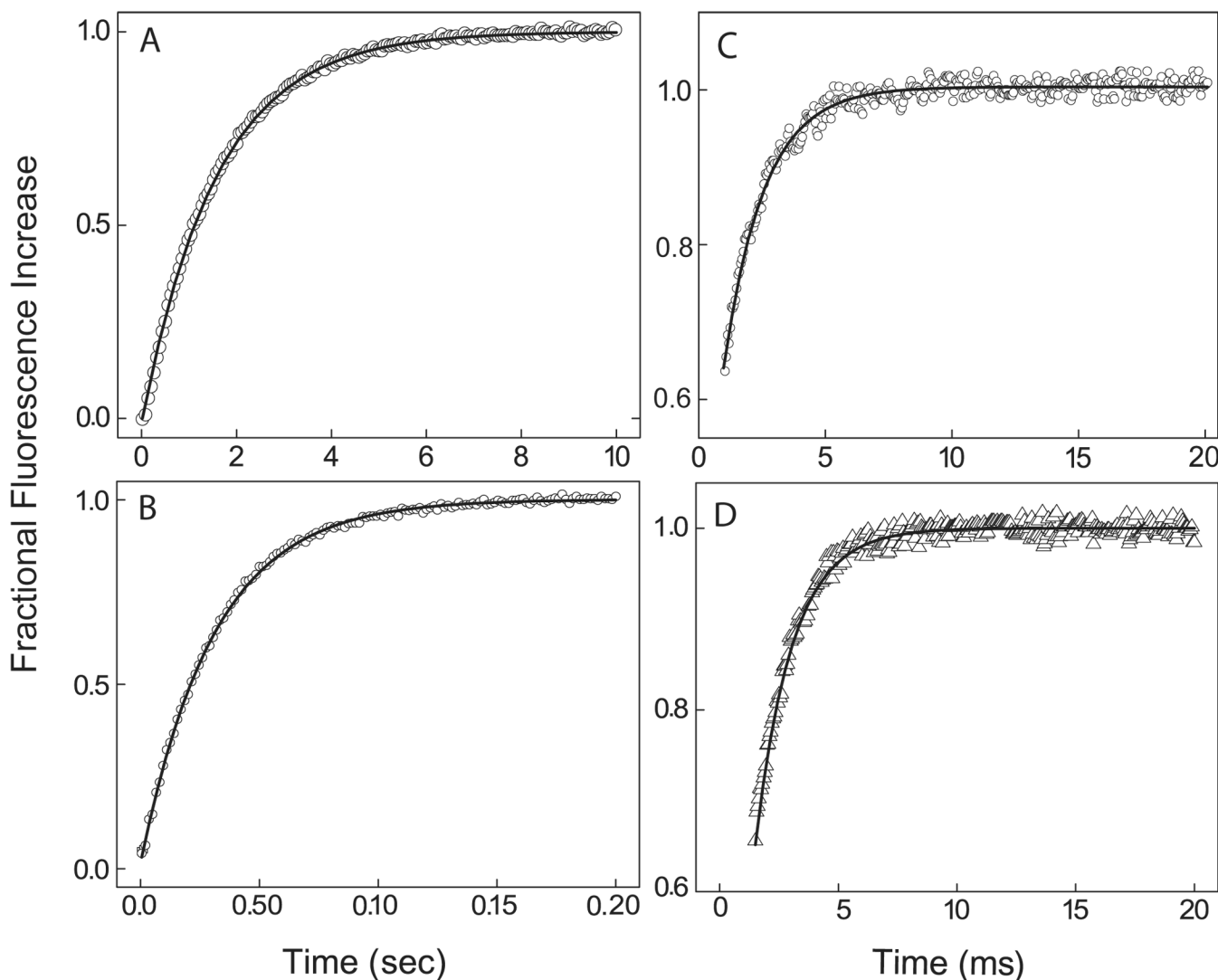


**Fig. 2. Dissociation of complexes between native and mutant CaMs and BSCaMIQ in the presence of CaM-binding peptides**

In all cases a range of peptide concentrations was investigated to ensure that a concentration sufficient to prevent rebinding of CaM was used. **(A)** Dissociation of the  $\text{Ca}^{2+}$ -free CaM-BSCaMIQ complex after addition of a peptide (ngPEP) based on the CaM-binding domain in neurogranin. Nominally  $\text{Ca}^{2+}$ -free conditions were produced by including 3 mM BAPTA in all experimental buffers. The final BSCaMIQ and CaM concentrations were 10 and 1  $\mu\text{M}$ ; the final peptide concentration was 100  $\mu\text{M}$ . The  $k_{\text{off}}$  value derived from mono-exponential fits to these and similar data is  $0.8 \pm 0.2 \text{ s}^{-1}$ . **(B)** Dissociation of the  $\text{NC}_x\text{CaM}$ -BSCaMIQ complex in the presence of 250  $\mu\text{M}$   $\text{CaCl}_2$  after addition of a peptide (ckPEP) based on the CaM-binding domain in CaM kinase II. The final BSCaMIQ and  $\text{N}_x\text{CCaM}$  concentrations were 50 and 10  $\mu\text{M}$ ; the final ckPEP concentration was 100  $\mu\text{M}$ . The dissociation rate constant derived from fits to these and similar data to single exponentials is  $30.2 \pm 4.2 \text{ s}^{-1}$ . **(C)** Dissociation of CaM-BSCaMIQ complex in the presence of 250  $\mu\text{M}$   $\text{CaCl}_2$  after addition of ckPEP at a final concentration of 100  $\mu\text{M}$ . The final BSCaMIQ and CaM concentrations were 12.5 and 2.5  $\mu\text{M}$ . The apparent dissociation rate constant derived from fits to these and similar data to single exponentials is  $565.1 \pm 13.1 \text{ s}^{-1}$ . **(D)** Dissociation of the  $\text{Ca}^{2+}$ -saturated  $\text{N}_x\text{CCaM}$ -BSCaMIQ

complex in the presence of 250  $\mu\text{M}$   $\text{CaCl}_2$  after addition of ckPEP at a final concentration of 100  $\mu\text{M}$ . The final BSCaM<sub>IQ</sub> and N<sub>x</sub>CCaM concentrations were 25 and 5  $\mu\text{M}$ . The apparent dissociation rate constant derived from fits of these and similar data to single exponentials is  $630.7 \pm 16.4 \text{ s}^{-1}$ .

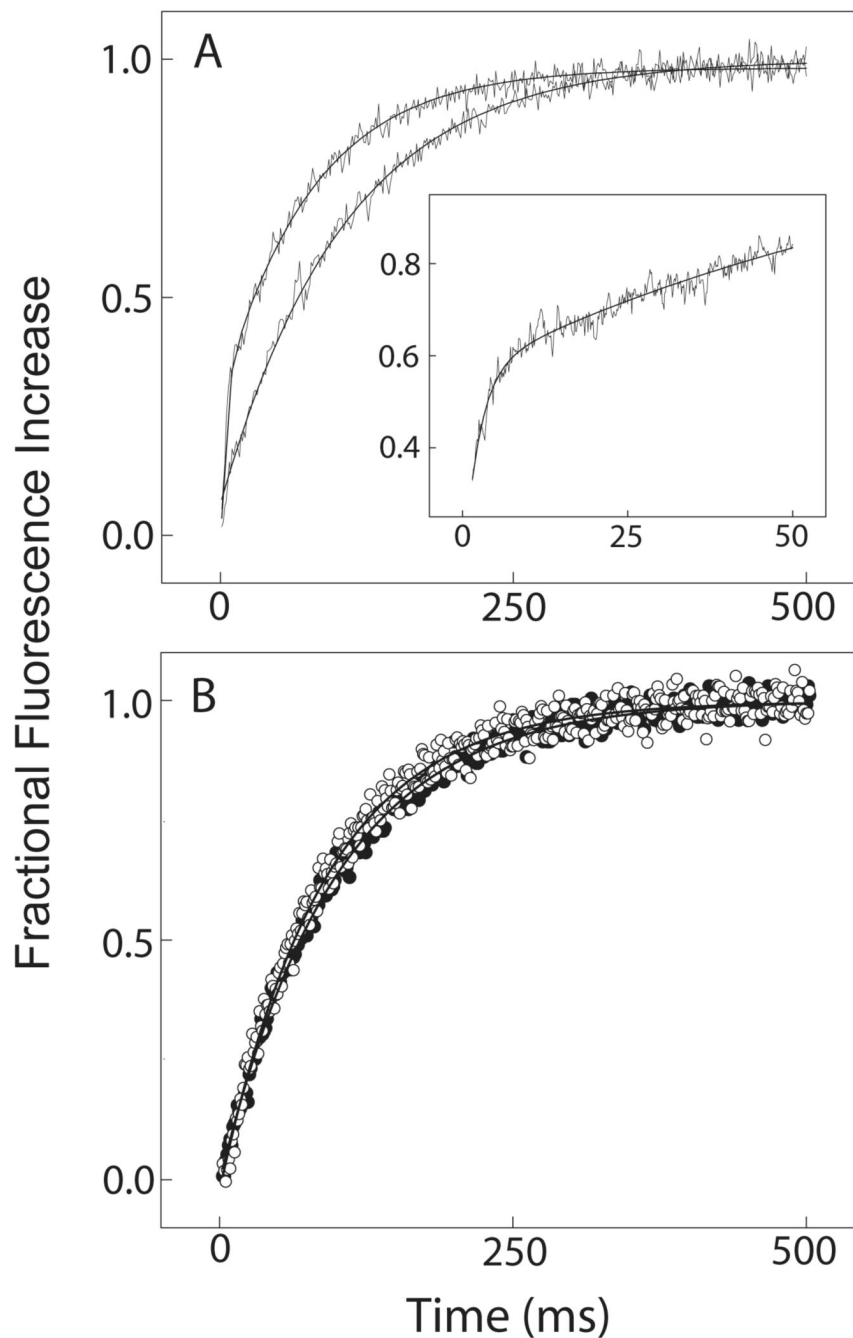


**Fig. 3. Dissociation of  $\text{Ca}^{2+}$  from the complex between BSCaMIQ and CaM or  $\text{N}_x\text{CCaM}$**   
 The fluorescent  $\text{Ca}^{2+}$  chelator quin-2 was used as a  $\text{Ca}^{2+}$  trap. Dissociation of  $\text{Ca}^{2+}$  from native or mutant CaM therefore corresponds directly with a  $\text{Ca}^{2+}$ -dependent increase in quin-2 fluorescence. A range of quin-2 concentrations was investigated to ensure that a concentration sufficient to prevent rebinding of  $\text{Ca}^{2+}$  was used. **(A)** Dissociation of  $\text{Ca}^{2+}$  from free CaM (lower trace) and from the CaM-BSCaMIQ complex (upper trace). The quin-2 fluorescence time course for  $\text{Ca}^{2+}$  dissociation from free CaM was generated by mixing a solution containing  $4 \mu\text{M}$  CaM and  $50 \mu\text{M}$   $\text{CaCl}_2$  with an equal volume of  $400 \mu\text{M}$  quin-2. These data are fit by a single exponential with a rate constant of  $10.3 \pm 0.7 \text{ s}^{-1}$  and an amplitude corresponding with dissociation of  $\sim 2 \text{ Ca}^{2+}$  ions. Dissociation of two additional  $\text{Ca}^{2+}$  ions occurred within the



instrument dead time. The quin-2 fluorescence time course for  $\text{Ca}^{2+}$  dissociation from the CaM-BSCaM<sub>IQ</sub> complex was generated by mixing a solution containing 25  $\mu\text{M}$  BSCaM<sub>IQ</sub>, 4  $\mu\text{M}$  CaM and 50  $\mu\text{M}$   $\text{CaCl}_2$  with an equal volume of 400  $\mu\text{M}$  quin-2. The data presented are fit by a double exponential. The slower process has an apparent rate constant of  $14.7 \pm 0.5 \text{ s}^{-1}$  and an amplitude corresponding with dissociation of  $\sim 2 \text{ Ca}^{2+}$  ions. The faster rate was derived from data measured over a shorter time interval (inset). These data are fit by a double exponential with rate constants of  $427.4 \pm 35$  and  $11.7 \pm 0.5 \text{ s}^{-1}$ , and respective amplitudes corresponding with dissociation of  $\sim 1.5$  and  $\sim 2 \text{ Ca}^{2+}$  ions. If the faster process is forced to have an amplitude corresponding with dissociation of 2  $\text{Ca}^{2+}$  ions, then apparent rate constants of  $473.4 \pm 37.9 \text{ s}^{-1}$  and  $12.9 \pm 0.7 \text{ s}^{-1}$  are derived for the faster and slower rates. **(B)** Dissociation of  $\text{Ca}^{2+}$  from the  $\text{N}_x\text{CCaM-BSCaM}_{IQ}$  complex ( $\bullet$ ) and from free  $\text{N}_x\text{CCaM}$  ( $\circ$ ). For these experiments a solution containing 4  $\mu\text{M}$   $\text{N}_x\text{CCaM}$  and 50  $\mu\text{M}$   $\text{CaCl}_2$  in the presence or absence of 25  $\mu\text{M}$  BSCaM<sub>IQ</sub> was mixed with an equal volume of 400  $\mu\text{M}$  quin-2. The two resulting quin-2 fluorescence time courses are essentially superimposable.  $\text{Ca}^{2+}$ -dissociation rate constants of  $10.8 \pm 0.6 \text{ s}^{-1}$  and  $11.8 \pm 0.5 \text{ s}^{-1}$  were derived for free and bound  $\text{N}_x\text{CCaM}$  from fits of these data to single exponentials with amplitudes corresponding to dissociation of  $\sim 2 \text{ Ca}^{2+}$  ions.

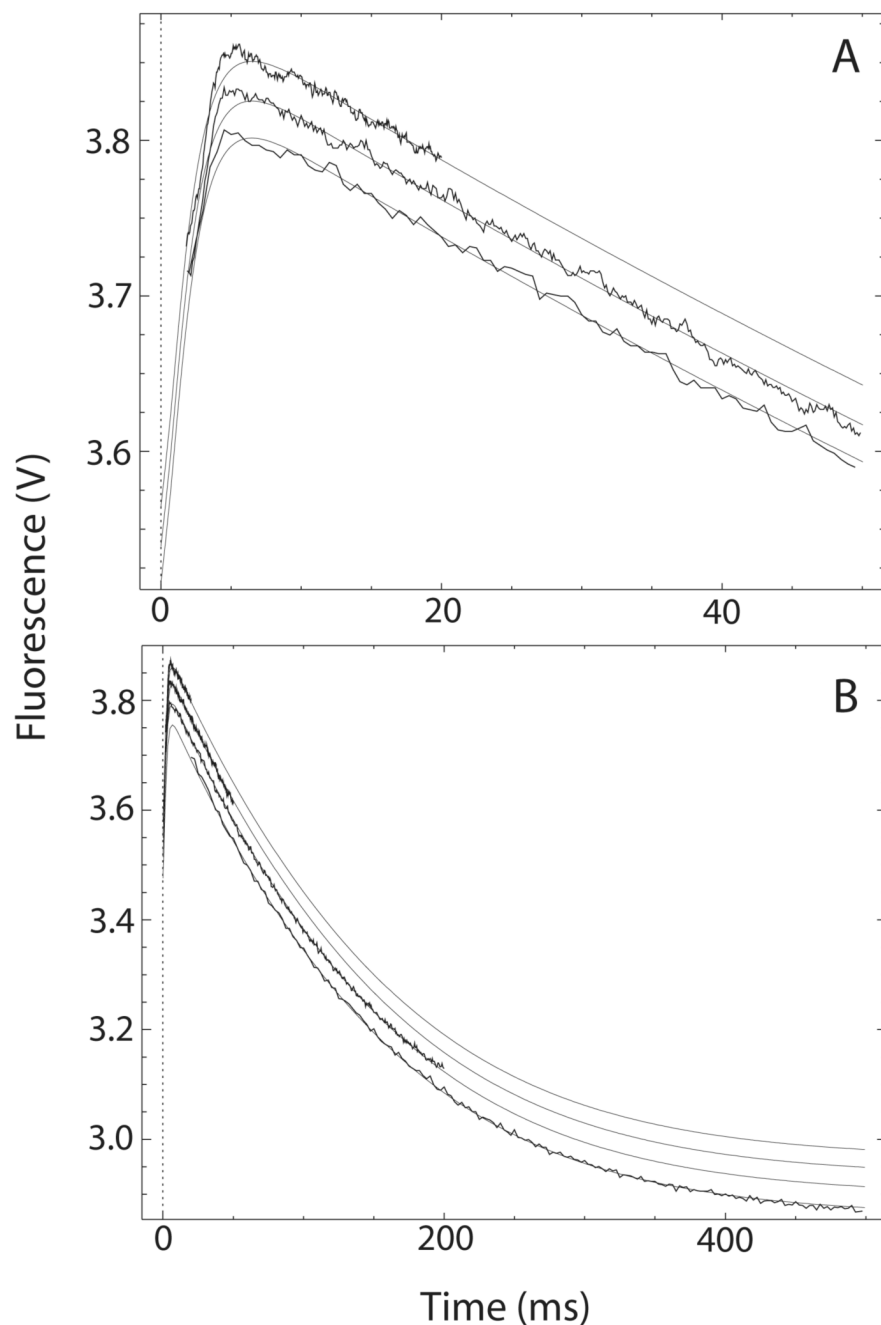


**Fig. 4. The transition from  $\text{Ca}^{2+}$ -saturated to  $\text{Ca}^{2+}$ -free CaM-BSCaM<sub>1Q</sub> complex**  
**(A, B)** Buffer containing 48  $\mu\text{M}$  CaM and 4  $\mu\text{M}$  BSCaM<sub>1Q</sub> in 500  $\mu\text{M}$   $\text{CaCl}_2$  was rapidly mixed with an equal volume of buffer containing 10 mM BAPTA. Data measured over 20, 50 and 200 ms time intervals are presented in panels A and B. Data measured over a 500 ms time interval are included in panel B. The individual data sets are offset on the y axis for presentation purposes. These data were globally fit to the model presented in Scheme 2 by iteratively varying the values for  $k'_{-2}$  and  $k'_{-4}$ , the  $\text{Ca}^{2+}$  dissociation rate constants for bound CaM, using the DynaFit program (18). Relative molar fluorescence amplitudes were assigned to the various kinetic species as detailed under “Materials and Methods”. Association and dissociation rate constants applied to the various  $\text{Ca}^{2+}$ -bound forms of the CaM-BSCaM<sub>1Q</sub> complex are given

in Table 1.  $\text{Ca}^{2+}$  dissociation rate constants applied to free CaM are given in Table 2. Parameters assigned to the  $\text{NC}_2\text{-B}$  species were determined using  $\text{N}_x\text{CCaM}$ . No attempt was made to include the standard errors associated with fixed parameter values. Steps marked as fast were arbitrarily assigned rates 10-fold faster than the steps preceding them. The fitted values obtained for  $k'_{-4}$  and  $k'_{-2}$  are  $528.3 \pm 3.3$  and  $13.5 \pm 0.1 \text{ s}^{-1}$ .

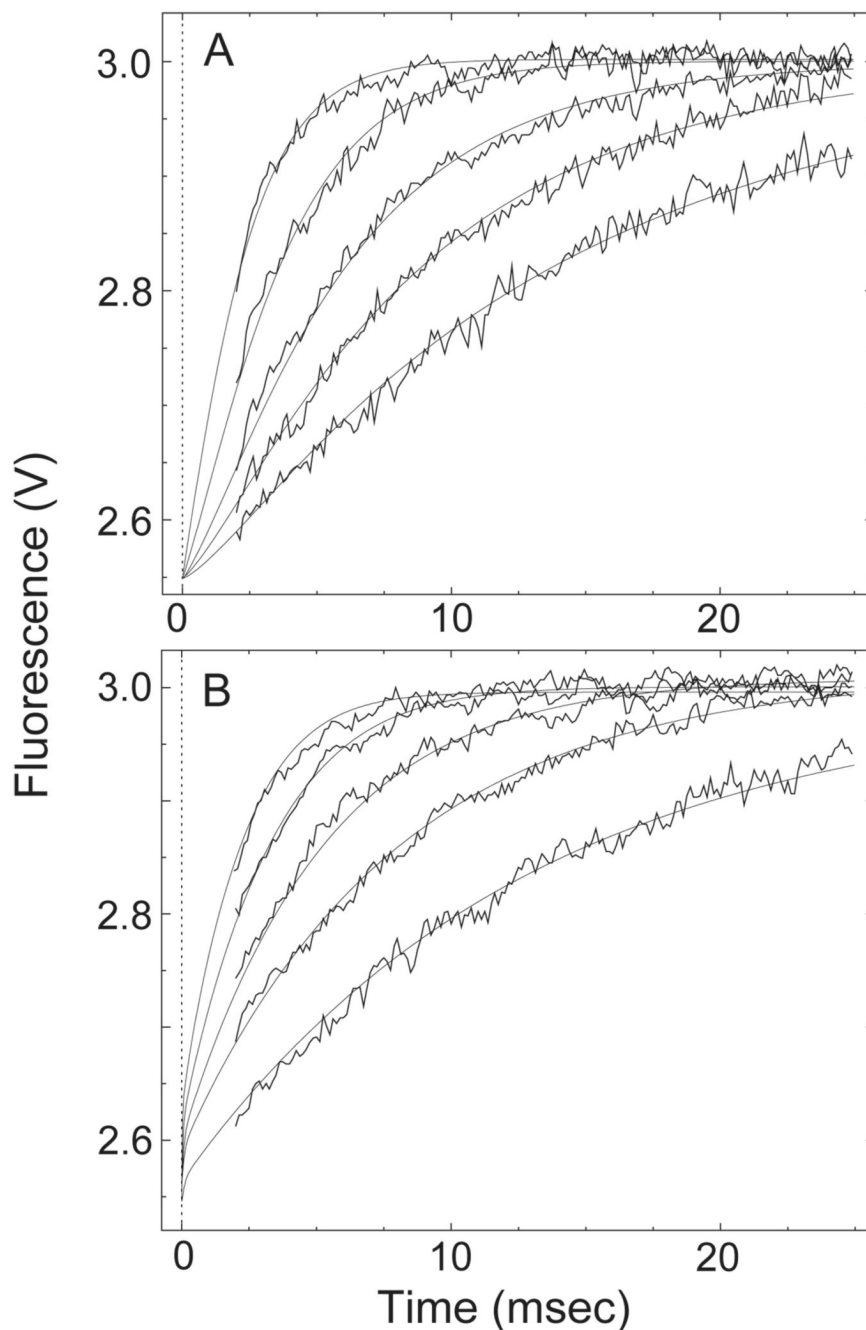
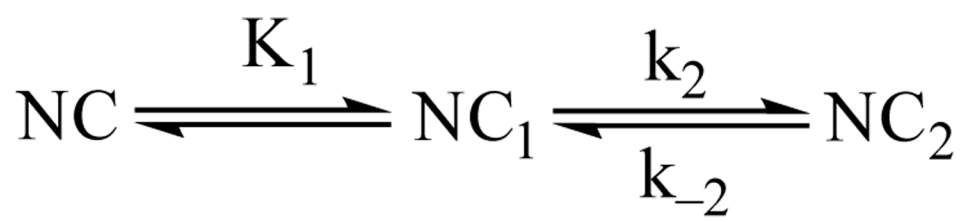


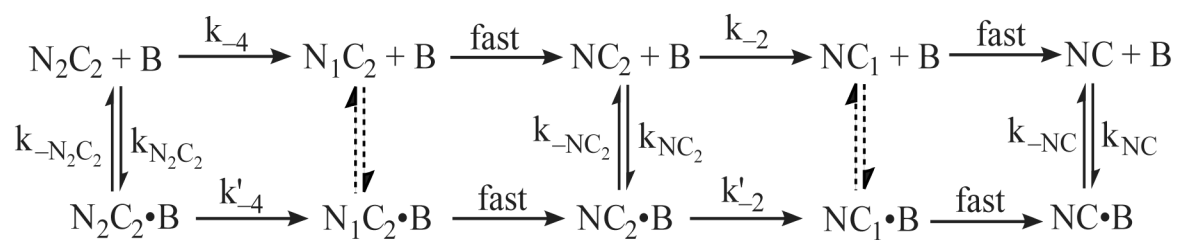
**Fig. 5. Dissociation of the initially  $\text{Ca}^{2+}$ -free complex between BSCaMIQ and native CaM or  $\text{N}_x\text{CCaM}$  after addition of  $\text{Ca}^{2+}$  and ckPEP**

Fluorescence data were measured after adding a solution containing 200  $\mu\text{M}$  ckPEP, along with  $\text{CaCl}_2$  in amounts producing the specified final concentrations, to an equal volume of a decalcified solution containing 20  $\mu\text{M}$  BSCaMIQ and either 4  $\mu\text{M}$  native CaM or  $\text{N}_x\text{CCaM}$ . (A) Dissociation of the  $\text{N}_x\text{CCaM}$ -BSCaMIQ complex in the presence of ckPEP with  $\text{Ca}^{2+}$  at concentrations of 30, 45, 67.5, 125 or 250  $\mu\text{M}$  (lowermost to uppermost trace). These data were globally fit according to an abbreviated version of the model presented in Scheme 3 containing only the steps associated with formation and dissociation of  $\text{NC}_2\text{-B}$ . The fit shown was produced by iteratively varying the values for  $K_1$  and  $k_2$  using the DynaFit program (18).

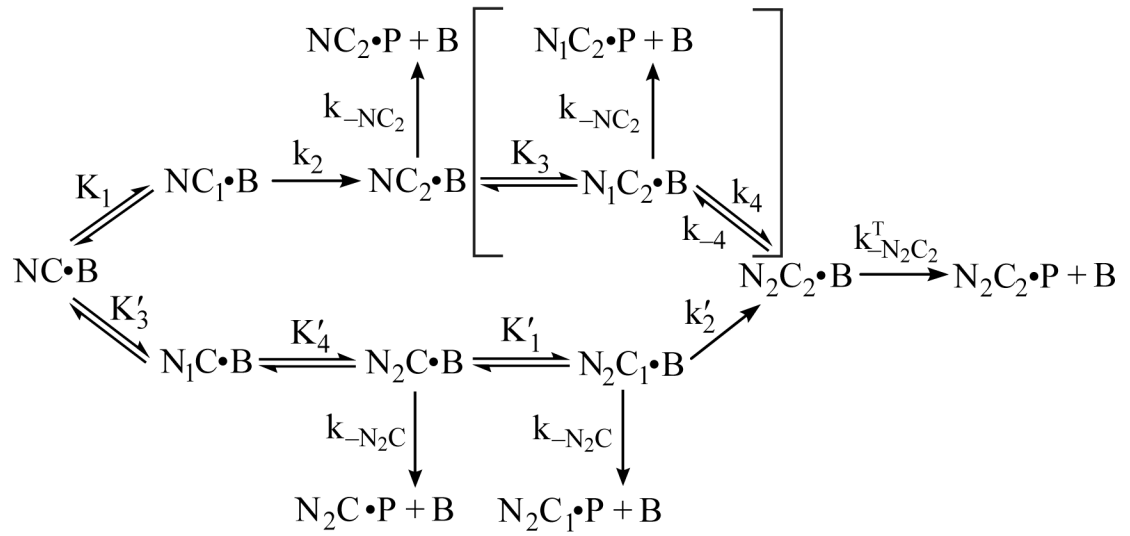
Relative molar fluorescence amplitudes were assigned to the various kinetic species as detailed under “Materials and Methods”. The dissociation rate constants assigned to the NC<sub>2</sub>-B species is given in Table 1. The NC-B species is effectively non-dissociating on this time scale. No attempt was made to include the standard errors associated with the fixed parameter value. The  $K_1$  and  $k_2$  values derived from the global fit shown are  $4.6 \pm 0.9 \mu\text{M}$  and  $3.1 \pm 0.1 \times 10^6 \text{ M}^{-1} \text{ s}^{-1}$ . **(B)** Dissociation of the native CaM-BSCaM<sub>IQ</sub> complex in the presence of ckPEP with Ca<sup>2+</sup> at a concentrations of 30, 45, 67.5, 125 or 250  $\mu\text{M}$  (lowermost to uppermost trace). Fluorescence time courses were globally fit according to the model presented in Scheme 3 by iteratively varying the values for  $K'_1$  and  $k'_2$  using the DynaFit program (18). Previously determined values of 122 and 9.4  $\mu\text{M}$  were assigned to  $K'_3$  and  $K'_4$  (15). The dissociation rate constants assigned to the NC-B, N<sub>2</sub>C-B, NC<sub>2</sub>-B and N<sub>2</sub>C<sub>2</sub>-B species are given in Table 1. The values used for the N<sub>2</sub>C-B and NC<sub>2</sub>-B species were determined using N<sub>x</sub>CCaM and NC<sub>x</sub>CaM. Values of  $4.6 \pm 0.9 \mu\text{M}$  and  $3.1 \pm 0.1 \times 10^6 \text{ M}^{-1} \text{ s}^{-1}$ , which were determined using N<sub>x</sub>CCaM, were assigned to  $K_1$  and  $k_2$  (Table 2). Relative molar fluorescence amplitudes were assigned to the various kinetic species as detailed under “Materials and Methods”. The  $K'_1$  and  $k'_2$  values derived from the global fit shown are  $4.1 \pm 0.6 \mu\text{M}$  and  $3.2 \pm 0.1 \times 10^6 \text{ M}^{-1} \text{ s}^{-1}$ .



SCHEME 1.



SCHEME 2.



SCHEME 3.



### Association and dissociation rate constants for native and mutant CaM-BSCaM<sub>IQ</sub> complexes

The first two columns contain  $k_{on}$  and  $k_{off}$  values derived from linear least-squares fits to replots of  $k_{obs}$  vs [CaM] (see Fig. 1).  $K_d$  values calculated using these rate constants are consistent with previously determined equilibrium  $K_d$  values (15). The last column contains  $k_{off}$  values derived from dissociation time courses measured in the presence of larger molar excesses of ngPEP or ckPEP (see Fig. 2).

Table 1

	$k_{obs}$ vs [CaM] plot	$k_{off}/k_{on}$	Equil	Peptide trap
CaM	$k_{on} (M^{-1}s^{-1})$ $k_{off} (s^{-1})$	$K_d (\mu M)$	$K_d (\mu M)$	$k_{off} (s^{-1})$
NC	$3.6 \pm 0.2 \times 10^5$ $0.9 \pm 0.2$	$2.5 \pm 0.6$	$2.3 \pm 0.1$	$0.8 \pm 0.2$
N <sub>1</sub> C	$3.9 \pm 0.6 \times 10^5$ $1.1 \pm 0.3$	$2.8 \pm 0.7$	$2.1 \pm 0.2$	$0.9 \pm 0.2$
N <sub>2</sub> C	$2.9 \pm 0.5 \times 10^5$ $0.9 \pm 0.2$	$3.1 \pm 0.9$	$2.5 \pm 0.3$	$0.7 \pm 0.3$
N <sub>3</sub> C <sub>1</sub>	$4.1 \pm 0.2 \times 10^5$ $558.8 \pm 10.1$	$13.6 \pm 1.1$	$14.4 \pm 1.3$	$630.7 \pm 16.4$
N <sub>2</sub> C <sub>2</sub>	$1.1 \pm 0.2 \times 10^6$ $30.9 \pm 1.6$	$28.1 \pm 5.3$	$36.7 \pm 3.9$	$30.2 \pm 4.2$
N <sub>2</sub> C <sub>3</sub>	$3.1 \pm 0.2 \times 10^6$ $69.4 \pm 9.6$	$2.2 \pm 0.3$	$2.5 \pm 0.1$	$565.1 \pm 13.1$

**Table 2****Ca<sup>2+</sup> association and dissociation rate constants for native and mutant CaMs free in solution or bound to BSCaM<sub>IQ</sub>**

Ca<sup>2+</sup> binding was modeled according to a sequential mechanism with a rapidly equilibrating first step (Scheme 1), so these rate constants correspond with the second Ca<sup>2+</sup>-binding step. Values indicated by an “NA” are not applicable; those indicated by an “ND” are too fast to measure in the stopped-flow fluorometer, which has a dead-time of ~1.4 ms. Association rate constants ( $k_{on}$ ) designated by a superscript “A” were calculated using the dissociation rate constants ( $k_{off}$ ) given in this table and previously determined equilibrium constants for the second Ca<sup>2+</sup> binding step (15). Association rate constants for the C-ter EF hand pair in the CaM-BSCaM<sub>IQ</sub> complex were derived from a global analysis of the fluorescence time courses presented in Fig. 5.  $k_{off}$  values designated by a superscript “B” were determined using a 5  $\mu$ l observation cell, which reduces the stopped-flow dead time to below 1 ms, but unfortunately cannot be used with solutions containing BSCaM<sub>IQ</sub> due to their higher viscosity.  $k_{off}$  values for the CaM-BSCaM<sub>IQ</sub> complex given in parenthesis were derived from a global analysis the fluorescence time courses presented in Fig. 4. All other  $k_{off}$  values were derived from quin-2 fluorescence data (Fig. 3).

CaM	N-ter EF hand pair		C-ter EF hand pair	
	$k_{on}$ ( $M^{-1}s^{-1}$ )	$k_{off}$ ( $s^{-1}$ )	$k_{on}$ ( $M^{-1}s^{-1}$ )	$k_{off}$ ( $s^{-1}$ )
NC	$3.1 \pm 1.2 \times 10^8$ <sup>A</sup>	$1152 \pm 117$ <sup>B</sup>	$3.4 \pm 2.4 \times 10^7$ <sup>A</sup>	$10.3 \pm 0.7$
N <sub>2</sub> C	NA	NA	$5.8 \pm 3.2 \times 10^7$ <sup>A</sup>	$10.8 \pm 0.6$
NC <sub>x</sub>	$3.4 \pm 1.5 \times 10^8$ <sup>A</sup>	$1298 \pm 135$ <sup>B</sup>	NA	NA
CaM-BSCaM <sub>IQ</sub>	$k_{on}$ ( $M^{-1}s^{-1}$ )	$k_{off}$ ( $s^{-1}$ )	$k_{on}$ ( $M^{-1}s^{-1}$ )	$k_{off}$ ( $s^{-1}$ )
NC	$3.0 \pm 1.2 \times 10^8$ <sup>A</sup>	$473.4 \pm 37.9$ ( $528.3 \pm 3.3$ )	$3.2 \pm 0.1 \times 10^6$	$11.7 \pm 0.5$ ( $13.5 \pm 0.1$ )
N <sub>2</sub> C	NA	NA	$3.1 \pm 0.1 \times 10^6$	$11.8 \pm 0.5$
NC <sub>x</sub>	ND	ND	NA	NA